

The Extended Kalman Filter for State Estimation of Dynamic UV Flash Processes[★]

Tobias K. S. Ritschel, John Bagterp Jørgensen

*Department of Applied Mathematics and Computer Science &
Center for Energy Resources Engineering (CERE),
Technical University of Denmark, DK-2800 Kgs. Lyngby, Denmark*

Abstract: We present an extended Kalman filter for state estimation of semi-explicit index-1 differential-algebraic equations. It is natural to model dynamic UV flash processes with such differential-algebraic equations. The UV flash is a mathematical statement of the second law of thermodynamics. It is therefore important to thermodynamically rigorous models of many phase equilibrium processes. State estimation of UV flash processes has applications in control, prediction, monitoring, and fault detection of chemical processes in the oil and gas industry, e.g. separation, distillation, drilling of oil wells, multiphase flow in oil pipes, and oil production. We present a numerical example of a UV flash separation process. It involves soft sensing of vapor-liquid compositions based on temperature and pressure measurements.

Keywords: Extended Kalman filter, State estimation, UV flash, Differential-algebraic equations

1. INTRODUCTION

State estimation is concerned with reconstructing the state of a process based on noisy measurements and a model of the process. It is central to nonlinear model predictive control, prediction, monitoring, and fault detection of several chemical processes in the oil and gas industry. For instance, authors have considered state estimation of distillation columns (Pan et al., 2009; Kataria et al., 2016), oil and gas pipe flow (Binder et al., 2015), oil well drilling (Nikoofard et al., 2017), and oil reservoir production (Oliver and Chen, 2011).

Many chemical processes involve phase equilibrium, i.e. thermodynamic equilibrium between two or more phases. The condition of phase equilibrium is derived from the second law of thermodynamics which states that the entropy of a closed system in equilibrium is maximal. The UV flash problem is a mathematical statement of the second law of thermodynamics. It is therefore a key component in thermodynamically rigorous models of phase equilibrium processes, e.g. flash separation (Castier, 2010; Arendsen and Versteeg, 2009; Lima et al., 2008), distillation columns (Flatby et al., 1994), and computational fluid dynamical problems (Hammer and Morin, 2014; Qiu et al., 2014). The UV flash problem can be formulated as an optimization problem (Michelsen, 1999). The solution to the optimization problem is the temperature, pressure, and phase compositions that maximize entropy. The optimization problem contains equality constraints on internal energy, U , volume, V , and total mass of each chemical component, n . U , V , and n are parameters in the optimization problem. The phase equilibrium conditions are the optimality

conditions of the optimization problem which are algebraic equations. Dynamical UV flash processes are therefore modeled with differential-algebraic equations (DAEs). Recently, Ritschel et al. (2017a) developed dynamic optimization algorithms for UV flash processes. However, state estimation of dynamic UV flash processes has not been treated in the open literature.

The Kalman filter is optimal for linear systems. However, many chemical processes are inherently nonlinear such that the Kalman filter cannot be used. There exist a number of nonlinear filters, e.g. the extended Kalman filter, the unscented Kalman filter, and particle filters (Simon, 2006). The extended Kalman filter applies the Kalman filter equations to a linearization of the nonlinear model. For highly nonlinear processes, this linearization can limit the accuracy of the extended Kalman filter. The unscented Kalman filter and particle filters use samples of the states to provide better estimates than the extended Kalman filter for severely nonlinear processes. The unscented Kalman filter uses deterministic samples whereas particle filters use random samples. A particular particle filter, called the ensemble Kalman filter, has gained much attention in oceanography and oil reservoir characterization (Evensen, 2009a,b; Gillijns et al., 2006). Alternatives to the above state estimation algorithms include moving-horizon estimation (Alessandri et al., 2010), which is an optimization-based algorithm, and neural network-based algorithms (Talebi et al., 2010). Research on state estimation algorithms was originally focused on systems of ordinary differential equations (ODEs). However, many processes are naturally modeled with DAEs. Algebraic equations often result from the approximation of a fast process as a quasi-steady-state, e.g. it is common to assume that phase equilibrium occurs instantaneously in dy-

[★] This project is funded by Innovation Fund Denmark in the OPTION project (63-2013-3).

dynamic processes. Recently, several authors have developed algorithms for state estimation of DAE models, e.g. the extended Kalman filter (Mobed et al., 2016; Jørgensen et al., 2007; Becerra et al., 2001), the unscented Kalman filter (Purohit et al., 2015, 2013; Pastorino et al., 2013; Mandela et al., 2010, 2009), particle filters (Haßkerl et al., 2017, 2016), and the ensemble Kalman filter (Puranik et al., 2012).

In this work, we present an extended Kalman filter for state estimation of dynamic UV flash processes. Such processes are modeled with DAEs in a semi-explicit index-1 form where the right-hand side of the differential equations are independent of the differential states. We exploit this fact in the computations. We present a numerical example that involves soft sensing of vapor-liquid compositions in a UV flash separation process based on temperature and pressure measurements.

The remainder of this paper is structured as follows. In Section 2, we describe the stochastic semi-explicit index-1 DAE system that we consider, and in Section 3, we describe the numerical simulation of such systems. In Section 4, we describe the extended Kalman filter. We briefly describe the model of the UV flash separation process in Section 5, and we present numerical results in Section 6. In Section 7, we present conclusions.

2. STOCHASTIC SEMI-EXPLICIT INDEX-1 DAE SYSTEMS

We consider stochastic DAE systems in the form

$$G(x(t), y(t), z(t)) = 0, \quad (1a)$$

$$dx(t) = F(y(t), u(t))dt + \sigma(y(t), u(t))d\omega(t). \quad (1b)$$

$x(t)$ is the state vector, $y(t)$ is a vector of algebraic variables, and $z(t)$ is a vector of adjoint algebraic variables. Phase equilibrium conditions can be formulated as the Karush-Kuhn-Tucker (KKT) conditions of an optimization problem. The algebraic equations (1a) represent such KKT conditions, and $z(t)$ represents the corresponding Lagrange multipliers. The stochastic differential equations (1b) represent conservation equations, and the states represent the conserved quantities. The right-hand side of the stochastic differential equations is independent of the states. The initial states are distributed as $x(t_0) \sim N(x_0, P_0)$. $u(t)$ are manipulated inputs, and $\omega(t)$ is a standard Wiener process, i.e. it has an incremental covariance of Idt . For the systems that we consider, the algebraic equations (1a) can be solved for $y(t)$ and $z(t)$ when $x(t)$ is given, i.e. the DAE system (1) is of index 1. The system is observed at discrete times, t_k , using the measurement equation,

$$y^m(t_k) = H(y(t_k)) + v(t_k). \quad (2)$$

$y^m(t_k)$ are the measurements. The right-hand side of the measurement equation is independent of the states. The measurement noise, $v(t_k)$, is normally distributed, i.e. $v(t_k) = v_k \sim N(0, T_k)$.

3. NUMERICAL SIMULATION

In this section, we describe the numerical simulation of the stochastic DAE system (1). We solve the differential equations and the algebraic equations in a simultaneous

manner. We discretize the deterministic and stochastic part of the stochastic differential equations (1b) with Euler's implicit and explicit method, respectively. That results in the equation $D_{k+1} = 0$ where

$$\begin{aligned} D_{k+1} &= D_{k+1}(x_{k+1}, y_{k+1}) = D_{k+1}(x_{k+1}, y_{k+1}; x_k, y_k, u_k) \\ &= x_{k+1} - F(y_{k+1}, u_k)\Delta t_k - \sigma(y_k, u_k)\Delta\omega_k - x_k. \end{aligned} \quad (3)$$

We introduce $w_{k+1} = [x_{k+1}; y_{k+1}; z_{k+1}]$. For each time step, we solve the residual equations, $R_{k+1} = 0$, for w_{k+1} . The residual function is

$$\begin{aligned} R_{k+1} &= R_{k+1}(w_{k+1}) = R_{k+1}(x_{k+1}, y_{k+1}, z_{k+1}) \\ &= R_{k+1}(x_{k+1}, y_{k+1}, z_{k+1}; x_k, y_k, u_k) \\ &= \begin{bmatrix} D_{k+1}(x_{k+1}, y_{k+1}; x_k, y_k, u_k) \\ G(x_{k+1}, y_{k+1}, z_{k+1}) \end{bmatrix}. \end{aligned} \quad (4)$$

We solve the residual equations with Newton's method:

$$w_{k+1}^{m+1} = w_{k+1}^m + \Delta w_{k+1}^m. \quad (5)$$

In each Newton iteration, we solve the linear system

$$M\Delta w_{k+1}^m = -R_{k+1}(w_{k+1}^m), \quad (6)$$

where the iteration matrix, M , is

$$M \approx \frac{\partial R_{k+1}}{\partial w_{k+1}} = \begin{bmatrix} I & -\frac{\partial F}{\partial y}\Delta t_k & 0 \\ \frac{\partial G}{\partial x} & \frac{\partial G}{\partial y} & \frac{\partial G}{\partial z} \end{bmatrix}. \quad (7)$$

3.1 Efficient solution of the linear system

The main computational task in the solution of the linear system (6) is the factorization of the iteration matrix, M . Because of the identity matrix in the Jacobian in (7), we can obtain an explicit expression for Δx_{k+1}^m from (6):

$$\Delta x_{k+1}^m = \left(\frac{\partial F}{\partial y}\Delta t_k \right) \Delta y_{k+1}^m - D_{k+1}. \quad (8)$$

We use (6) and (8) to obtain a reduced linear system for Δy_{k+1}^m and Δz_{k+1}^m :

$$\bar{M} \begin{bmatrix} \Delta y_{k+1}^m \\ \Delta z_{k+1}^m \end{bmatrix} = \frac{\partial G}{\partial x} D_{k+1} - G(x_{k+1}^m, y_{k+1}^m, z_{k+1}^m). \quad (9)$$

The reduced iteration matrix, \bar{M} , is

$$\bar{M} \approx \begin{bmatrix} \frac{\partial G}{\partial y} + \frac{\partial G}{\partial x} \frac{\partial F}{\partial y} \Delta t_k & \frac{\partial G}{\partial z} \end{bmatrix}. \quad (10)$$

It is cheaper to factorize \bar{M} than M because \bar{M} is smaller.

4. THE EXTENDED KALMAN FILTER

The extended Kalman filter consists of a) a measurement-update that incorporates the current measurement and b) a time-update that propagates the state mean and its covariance through time in between measurements. The initial state estimate and its covariance are the mean and covariance of the initial states:

$$\hat{x}_{0|-1} = x_0, \quad (11a)$$

$$P_{0|-1} = P_0. \quad (11b)$$

4.1 Measurement-update

The one-step ahead prediction of the measurement, $\hat{y}_{k|k-1}^m$, and its approximate covariance matrix, $T_{k|k-1}$, are

$$\hat{y}_{k|k-1}^m = H(\hat{y}_{k|k-1}), \quad (12a)$$

$$T_{k|k-1} = C_k P_{k|k-1} C_k' + T_k. \quad (12b)$$

The one-step ahead estimate of the algebraic variables, $\hat{y}_{k|k-1}$, is available from the previous time-update. T_k is the covariance matrix of the measurement noise. The matrix C_k is

$$C_k = \frac{\partial H}{\partial x}(\hat{y}_{k|k-1}) = \frac{\partial H}{\partial y}(\hat{y}_{k|k-1}) \frac{\partial \hat{y}_{k|k-1}}{\partial \hat{x}_{k|k-1}}. \quad (13)$$

As we describe later, the one-step ahead estimates satisfy the algebraic equations, i.e. $G(\hat{x}_{k|k-1}, \hat{y}_{k|k-1}, \hat{z}_{k|k-1}) = 0$. We apply the implicit function theorem to the algebraic equations in order to compute $\frac{\partial \hat{y}_{k|k-1}}{\partial \hat{x}_{k|k-1}}$ and $\frac{\partial \hat{z}_{k|k-1}}{\partial \hat{x}_{k|k-1}}$:

$$\begin{bmatrix} \frac{\partial G}{\partial y} & \frac{\partial G}{\partial z} \end{bmatrix} \begin{bmatrix} \frac{\partial \hat{y}_{k|k-1}}{\partial \hat{x}_{k|k-1}} \\ \frac{\partial \hat{z}_{k|k-1}}{\partial \hat{x}_{k|k-1}} \end{bmatrix} = -\frac{\partial G}{\partial x}. \quad (14)$$

The partial derivatives of G in (14) are evaluated at $\hat{x}_{k|k-1}$, $\hat{y}_{k|k-1}$, and $\hat{z}_{k|k-1}$. The innovation error of the measurement is

$$e_k = y_k^m - \hat{y}_{k|k-1}^m, \quad (15)$$

where $y_k^m = y^m(t_k)$ is the measurement. The Kalman filter gain matrix is

$$K_{f,x,k} = P_{k|k-1} C_k' T_{k|k-1}^{-1}. \quad (16)$$

The filtered state and its approximate covariance matrix are updated by

$$\hat{x}_{k|k} = \hat{x}_{k|k-1} + K_{f,x,k} e_k, \quad (17a)$$

$$P_{k|k} = P_{k|k-1} - K_{f,x,k} T_{k|k-1} K_{f,x,k}'. \quad (17b)$$

The filtered estimates of the algebraic and adjoint algebraic variables satisfy the algebraic equations:

$$G(\hat{x}_{k|k}, \hat{y}_{k|k}, \hat{z}_{k|k}) = 0. \quad (18)$$

The corresponding approximate covariance matrices are

$$P_{y,k|k} = \Phi_{yx}(t_k, t_k) P_{k|k} \Phi_{yx}'(t_k, t_k), \quad (19a)$$

$$P_{z,k|k} = \Phi_{zx}(t_k, t_k) P_{k|k} \Phi_{zx}'(t_k, t_k). \quad (19b)$$

We use the implicit function theorem to compute the sensitivities, $\Phi_{yx}(t_k, t_k) = \frac{\partial \hat{y}_{k|k}}{\partial \hat{x}_{k|k}}$ and $\Phi_{zx}(t_k, t_k) = \frac{\partial \hat{z}_{k|k}}{\partial \hat{x}_{k|k}}$:

$$\begin{bmatrix} \frac{\partial G}{\partial y} & \frac{\partial G}{\partial z} \end{bmatrix} \begin{bmatrix} \Phi_{yx}(t_k, t_k) \\ \Phi_{zx}(t_k, t_k) \end{bmatrix} = -\frac{\partial G}{\partial x}. \quad (20)$$

The partial derivatives of G in (20) are evaluated at $\hat{x}_{k|k}$, $\hat{y}_{k|k}$, and $\hat{z}_{k|k}$.

4.2 Time-update

In the time-update, we propagate the state estimate and covariance matrix from time t_k to time t_{k+1} where the next measurement arrives. We obtain the one-step ahead predictions at time t_{k+1} by solving the initial value problem

$$\hat{x}_k(t_k) = \hat{x}_{k|k}, \quad (21a)$$

$$G(\hat{x}_k(t), \hat{y}_k(t), \hat{z}_k(t)) = 0, \quad t \in]t_k; t_{k+1}], \quad (21b)$$

$$\frac{d\hat{x}_k(t)}{dt} = F(\hat{y}_k(t), u(t)), \quad t \in]t_k; t_{k+1}]. \quad (21c)$$

The sensitivities, $\Phi_{xx}(t, s) = \frac{\partial \hat{x}_k(t)}{\partial \hat{x}_k(s)}$, $\Phi_{yx}(t, s) = \frac{\partial \hat{y}_k(t)}{\partial \hat{x}_k(s)}$, and $\Phi_{zx}(t, s) = \frac{\partial \hat{z}_k(t)}{\partial \hat{x}_k(s)}$, satisfy

$$\Phi_{xx}(s, s) = I, \quad (22a)$$

$$\frac{\partial G}{\partial x} \Phi_{xx}(t, s) + \frac{\partial G}{\partial y} \Phi_{yx}(t, s) + \frac{\partial G}{\partial z} \Phi_{zx}(t, s) = 0, \quad (22b)$$

$$\frac{d\Phi_{xx}(t, s)}{dt} = \frac{\partial F}{\partial y} \Phi_{yx}(t, s). \quad (22c)$$

The partial derivatives of F and G in (22) are evaluated at $\hat{x}_k(t)$, $\hat{y}_k(t)$, and $\hat{z}_k(t)$. We compute the covariance matrix from the sensitivities (Jørgensen et al., 2007):

$$P_k(t) = \Phi_{xx}(t, t_k) P_{k|k} \Phi_{xx}'(t, t_k) + \int_{t_k}^t \Phi_{xx}(t, s) \sigma(\hat{y}_k(s), u(s)) \sigma(\hat{y}_k(s), u(s))' \Phi_{xx}'(t, s) ds. \quad (23)$$

4.3 Numerical solution of the time-update equations

We use Euler's implicit method to solve the initial value problem (21) for the one-step ahead predictions, $\hat{x}_{k+1|k} = \hat{x}_k(t_{k+1})$, $\hat{y}_{k+1|k} = \hat{y}_k(t_{k+1})$, and $\hat{z}_{k+1|k} = \hat{z}_k(t_{k+1})$. That corresponds to solving the nonlinear equations

$$\begin{aligned} R_{k+1|k} &= R_{k+1|k}(\hat{x}_{k+1|k}, \hat{y}_{k+1|k}, \hat{z}_{k+1|k}) \\ &= R_{k+1|k}(\hat{x}_{k+1|k}, \hat{y}_{k+1|k}, \hat{z}_{k+1|k}; \hat{x}_{k|k}, u_k) \\ &= \begin{bmatrix} \hat{x}_{k+1|k} - F(\hat{y}_{k+1|k}, u_k) \Delta t_k - \hat{x}_{k|k} \\ G(\hat{x}_{k+1|k}, \hat{y}_{k+1|k}, \hat{z}_{k+1|k}) \end{bmatrix} = 0. \end{aligned} \quad (24)$$

We solve the nonlinear equations (24) with Newton's method. The approach is similar to the one described in Section 3. We also discretize the sensitivity equations (22) with Euler's implicit method:

$$\begin{bmatrix} I & -\frac{\partial F}{\partial y} \Delta t_k & 0 \\ \frac{\partial G}{\partial x} & \frac{\partial G}{\partial y} & \frac{\partial G}{\partial z} \end{bmatrix} \begin{bmatrix} \Phi_{xx}(t_{k+1}, t_k) \\ \Phi_{yx}(t_{k+1}, t_k) \\ \Phi_{zx}(t_{k+1}, t_k) \end{bmatrix} = \begin{bmatrix} I \\ 0 \end{bmatrix}. \quad (25)$$

The partial derivatives of F and G in (25) are evaluated at $\hat{x}_{k+1|k}$, $\hat{y}_{k+1|k}$, and $\hat{z}_{k+1|k}$. We exploit the structure of the linear system (25) in the same way that we did in Section 3.1. We discretize the integral in (23) with a left rectangle quadrature rule to obtain an expression for $P_{k+1|k} = P_k(t_{k+1})$:

$$P_{k+1|k} = \Phi_{xx}(t_{k+1}, t_k) \Lambda_k \Phi_{xx}'(t_{k+1}, t_k) \quad (26a)$$

$$\Lambda_k = P_{k|k} + \sigma(\hat{y}_{k|k}, u_k) \sigma(\hat{y}_{k|k}, u_k)' \Delta t_k \quad (26b)$$

5. DYNAMIC UV FLASH SEPARATION PROCESS

In this section, we consider a flash separation process where a mixture of N_C chemical components is separated into a vapor phase and a liquid phase. The vapor phase and the liquid phase are in thermodynamic equilibrium. A feed stream supplies the separator with a vapor-liquid mixture. The mixture exits the separator from a vapor stream and a liquid stream, and the separator is subject to external heating. The two main principles of the model of the separation process are 1) vapor-liquid equilibrium and 2) conservation of mass and energy.

5.1 Vapor-liquid equilibrium

The vapor phase (v) and the liquid phase (l) are in thermodynamic equilibrium. The second law of thermodynamics states that the entropy, S , of a closed system in equilibrium

is maximal. As we discuss later, the internal energy, U , and the total composition of the mixture (in moles), n , are given by conservation equations. The volume, V , of the separator is fixed. The above conditions constitute the UV flash optimization problem,

$$\max_{T,P,n^v,n^l} S = S^v(T,P,n^v) + S^l(T,P,n^l), \quad (27a)$$

$$\text{s.t.} \quad U^v(T,P,n^v) + U^l(T,P,n^l) = U, \quad (27b)$$

$$V^v(T,P,n^v) + V^l(T,P,n^l) = V, \quad (27c)$$

$$n_i^v + n_i^l = n_i, \quad i = 1, \dots, N_C. \quad (27d)$$

The solution to the UV flash optimization problem is the temperature, T , pressure, P , and vapor-liquid composition (in moles), n^v and n^l , that maximize entropy while satisfying the constraints on the internal energy, U , volume, V , and total composition, n . The UV flash is sometimes called the UVn flash or the isoenergetic-isochoric (constant energy - constant volume) flash. The UV flash optimization problem (27) is in the form

$$\min_y f(y), \quad (28a)$$

$$\text{s.t.} \quad g(y) = x, \quad (28b)$$

$$h(y) = 0, \quad (28c)$$

where the states are $x = [U; n]$, and the algebraic variables are $y = [T; P; n^v; n^l]$. Because (28) does not contain inequality constraints, the first-order optimality conditions are a set of algebraic equations:

$$G(x, y, z) = 0. \quad (29)$$

z are Lagrange multipliers.

5.2 Conservation of mass and energy

The internal energy, U , and the total composition (in moles), n , of the mixture are conserved. The deterministic conservation equations are

$$\dot{U}(t) = H_F^v(t) + H_F^l(t) - H_V(t) - H_L(t) + Q(t), \quad (30a)$$

$$\dot{n}_i(t) = f_{F,i}^v(t) + f_{F,i}^l(t) - v_i(t) - l_i(t), \quad i = 1, \dots, N_C. \quad (30b)$$

H_F^v and H_F^l are the vapor-liquid enthalpies of the feed stream, and H_V and H_L are the enthalpies of the vapor and liquid streams. Similarly, $f_{F,i}^v$ and $f_{F,i}^l$ are the vapor-liquid flow rates of the feed stream, and v_i and l_i are the flow rates of the vapor stream and the liquid stream. Q is the heat flux from the external heating. The deterministic conservation equations (30) are in the form

$$\dot{x}(t) = F(y(t), u(t)), \quad (31)$$

where u are inputs. Adding process noise to (31) results in the stochastic differential equations (1b).

5.3 Thermodynamic model

Because the vapor-liquid equilibrium conditions are the first-order optimality conditions of an optimization problem, they contain first-order derivatives of thermodynamic functions. We therefore need to evaluate second-order derivatives of thermodynamic functions in order to evaluate the Jacobian matrices of the equilibrium conditions. We use the open-source thermodynamic library, ThermoLib, developed by Ritschel et al. (2017b, 2016) for that purpose. It implements a thermodynamic model

based on the DIPPR database (Thomson, 1996) and cubic equations of state. It provides routines that evaluate enthalpy, $H = H(T, P, n)$, entropy, $S = S(T, P, n)$, and volume, $V = V(T, P, n)$, as well as first- and second-order derivatives. Given H , S , and V , the internal energy is $U = H - PV$, Gibbs energy is $G = H - TS$, and Helmholtz energy is $A = U - TS$. ThermoLib is available from www.psetools.org.

6. NUMERICAL EXAMPLE

We use the extended Kalman filter as a soft sensor that can estimate the vapor-liquid composition of a mixture based on temperature and pressure measurements. Soft sensing of compositions is an economical alternative to physical sensors which can be slow, expensive, and lack accuracy. We consider the separation of a mixture of 60% C_1 , 8% C_2 , 5% C_3 , 25% n- C_7 , and 2% CO_2 in a 0.2 m³ separator. We consider a 72 h time interval and a sampling time of 5 min. We assume that the inputs are known. The tank is cooled, i.e. $Q \leq 0$. Q increases from -9 MJ/h to -4 MJ/h after 24 h. The feed flow rate is constant at 1000 mol/h, and the vapor-liquid stream flow rates are constant at 400 mol/h and 600 mol/h. The standard deviations of the temperature and pressure measurement noise are 10 K and $10^{-1/2} \approx 0.3$ MPa. We consider a constant diffusion coefficient, i.e. $\sigma(y(t), u(t)) = \sigma = \text{diag}([\sigma_U; \sigma_{C_1}; \sigma_{C_2}; \sigma_{C_3}; \sigma_{n-C_7}; \sigma_{CO_2}])$, where $\sigma_U = 1$ MJ, $\sigma_{C_1} = \sigma_{C_2} = \sigma_{n-C_7} = 1$ mol, and $\sigma_{C_3} = \sigma_{CO_2} = 0.1$ mol. The mean of the initial states, x_0 , is a steady-state of the deterministic system (30), and the covariance of the initial states is $P_0 = \sigma\sigma'$.

Fig. 1 shows the filtered estimates of the total composition (in moles), internal energy, temperature, and pressure. It also shows the deviation of the estimates from the corresponding true simulated quantities and the root-mean-square deviation (RMSD). The RMSD of the i 'th state variable is

$$\text{RMSD}_i = \left(\frac{1}{N+1} \sum_{k=0}^N (\hat{x}_{i,k|k} - x_{i,k})^2 \right)^{1/2}, \quad (32)$$

where we compute the simulated states, x_k , as described in Section 3. $N+1 = 865$ is the number of measurement samples. The RMSD of the temperature and pressure estimates are computed similarly. We see that the deviations of the estimates are small compared to the scales of the estimates. Fig. 2 shows the filtered estimates of the total mole fractions, the vapor-liquid mole fractions, and the vapor fraction. Such estimates are necessary in model predictive control of processes with constraints on the purity (i.e. mole fractions) of the output streams, e.g. separation and distillation processes.

7. CONCLUSIONS

We present an extended Kalman filter for state estimation of UV flash processes. It is natural to model such processes, as well as other phase equilibrium processes, with DAEs that are in a semi-explicit index-1 form. We describe a model of a UV flash separation process, and demonstrate that it is in the semi-explicit index-1 DAE form. Finally, we demonstrate the accuracy of the extended Kalman

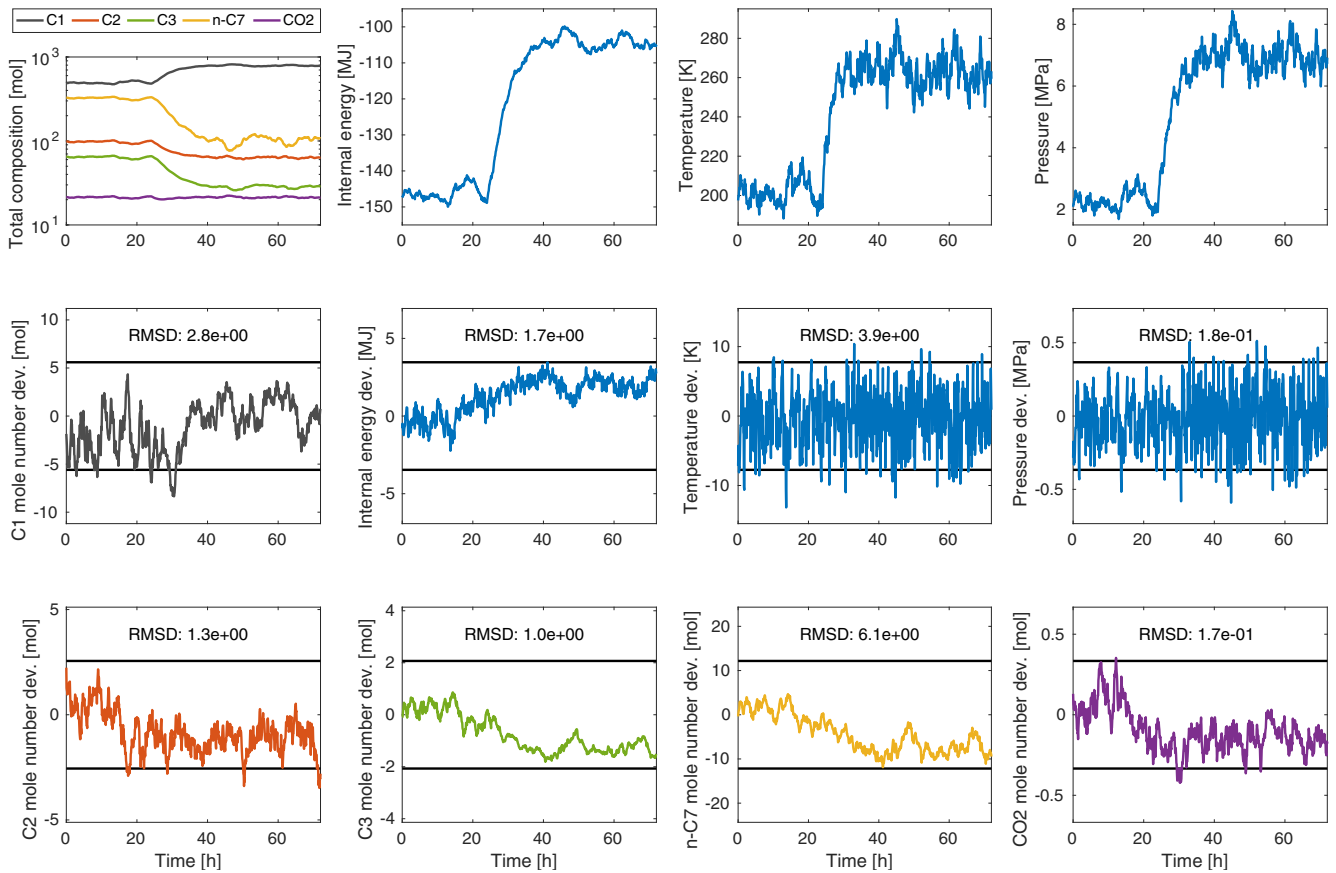


Fig. 1. Top row: filtered estimates of total composition, internal energy, temperature, and pressure. Middle and bottom rows: deviation (dev.) of estimates from the simulated (i.e. true) separation process. The black horizontal lines are \pm two times the RMSD of the estimates.

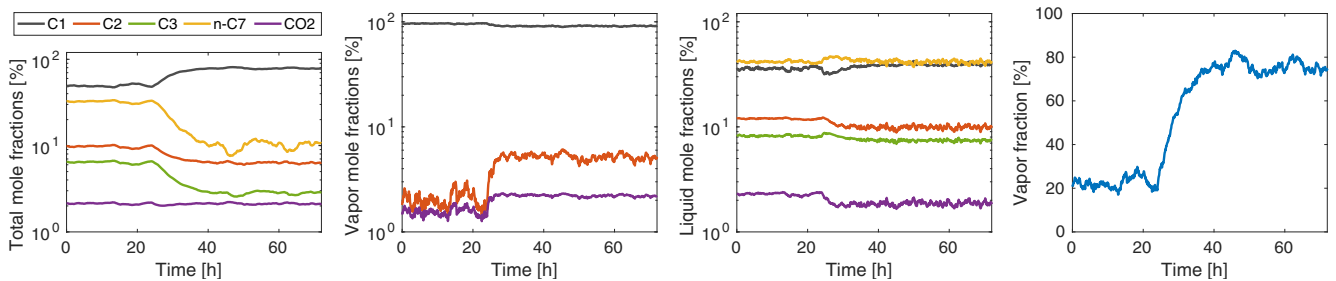


Fig. 2. Estimates of the total mole fractions, vapor mole fractions, liquid mole fractions, and the vapor fraction. We do not show the vapor mole fractions of C_3 and n-C7 because they are very small, i.e. below 1%.

filter with a numerical example that involves soft sensing of vapor-liquid compositions based on temperature and pressure measurements.

REFERENCES

- Alessandri, A., Baglietto, M., Battistelli, G., and Zavala, V. (2010). Advances in moving horizon estimation for nonlinear systems. In *Proceedings of the 49th IEEE Conference on Decision and Control*. Atlanta, Georgia, USA.
- Arendsen, A.R.J. and Versteeg, G.F. (2009). Dynamic thermodynamics with internal energy, volume, and amount of moles as states: Application to liquefied gas tank. *Industrial & Engineering Chemistry Research*, 48(6), 3167–3176.
- Becerra, V.M., Roberts, P.D., and Griffiths, G.W. (2001). Applying the extended Kalman filter to systems described by nonlinear differential-algebraic equations. *Control Engineering Practice*, 9(3), 267–281.
- Binder, B.J.T., Pavlov, A., and Johansen, T.A. (2015). Estimation of flow rate and viscosity in a well with an electric submersible pump using moving horizon estimation. In *Proceedings of the 2nd IFAC Workshop on Automatic Control in Offshore Oil and Gas Production*, 140–146. Florianópolis, Brazil.
- Castier, M. (2010). Dynamic simulation of fluids in vessels via entropy maximization. *Journal of Industrial and Engineering Chemistry*, 16(1), 122–129.
- Evensen, G. (2009a). *Data Assimilation. The Ensemble Kalman Filter*. Springer-Verlag Berlin Heidelberg, 2nd edition.

- Evensen, G. (2009b). The ensemble Kalman filter for combined state and parameter estimation. *IEEE Control Systems*, 29(3), 83–104.
- Flatby, P., Skogestad, S., and Lundström, P. (1994). Rigorous dynamic simulation of distillation columns based on UV-flash. In *IFAC Symposium on Advanced Control of Chemical Processes (ADCHEM '94)*, 261–266.
- Gillijns, S., Mendoza, O.B., Chandrasekar, J., De Moor, B.L.R., Bernstein, D.S., and Ridley, A. (2006). What is the ensemble Kalman filter and how well does it work? In *Proceedings of the 2006 American Control Conference*, 4448–4453. Minneapolis, Minnesota, USA.
- Hammer, M. and Morin, A. (2014). A method for simulating two-phase pipe flow with real equations of state. *Computers & Fluids*, 100, 45–58.
- Haßkerl, D., Arshad, M., Hashemi, R., Subramanian, S., and Engell, S. (2016). Simulation study of the particle filter and the EKF for state estimation of a large-scale DAE-system with multi-rate sampling. In *Proceedings of the 11th IFAC symposium on Dynamics and Control of Process Systems Including Biosystems*, 490–495. Trondheim, Norway.
- Haßkerl, D., Subramanian, S., Hashemi, R., Arshad, M., and Engell, S. (2017). State estimation using a multi-rate particle filter for a reactive distillation column described by a DAE model. In *Proceedings of the 25th Mediterranean Conference on Control and Automation*, 876–881. Valletta, Malta.
- Jørgensen, J.B., Kristensen, M.R., Thomsen, P.G., and Madsen, H. (2007). New extended Kalman filter algorithms for stochastic differential algebraic equations. In *Assessment and Future Directions of Nonlinear Model Predictive Control*, volume 358 of *Lecture Notes in Control and Information Sciences*, 359–366. Springer-Verlag Berlin Heidelberg.
- Kataria, G., Singh, K., and Dohare, R.K. (2016). ANN based soft sensor model for reactive distillation column. *International Journal of Advanced Technology and Engineering Exploration*, 3(24), 182–186.
- Lima, E.R.A., Castier, M., and Biscaia Jr., E.C. (2008). Differential-algebraic approach to dynamic simulations of flash drums with rigorous evaluation of physical properties. *Oil & Gas Science and Technology*, 63(5), 677–686.
- Mandela, R.K., Rengaswamy, R., and Narasimhan, S. (2009). Nonlinear state estimation of differential algebraic systems. In *Proceedings of the 7th IFAC Symposium on Advanced Control of Chemical Processes*, 792–797.
- Mandela, R.K., Rengaswamy, R., Narasimhan, S., and Sridhar, L.N. (2010). Recursive state estimation techniques for nonlinear differential algebraic systems. *Chemical Engineering Science*, 65(16), 4548–4556.
- Michelsen, M.L. (1999). State function based flash specifications. *Fluid Phase Equilibria*, 158–160, 617–626.
- Mobed, P., Munusamy, S., Bhattacharyya, D., and Rengaswamy, R. (2016). State and parameter estimation in distributed constrained systems. 1. extended Kalman filtering of a special class of differential-algebraic equation systems. *Industrial & Engineering Chemistry Research*, 56(1), 206–215.
- Nikoofard, A., Aarsnes, U.J.F., Johansen, T.A., and Kaasa, G.O. (2017). State and parameter estimation of a drift-flux model for underbalanced drilling operations. *IEEE Transactions on Control Systems Technology*, 25(6), 2000–2009.
- Oliver, D.S. and Chen, Y. (2011). Recent progress on reservoir history matching: a review. *Computational Geosciences*, 15(1), 185–221.
- Pan, S., Su, H., Li, P., and Gu, Y. (2009). State estimation for batch distillation operations with a novel extended Kalman filter approach. In *Proceedings of the Joint 48th Conference on Decision and Control and 28th Chinese Control Conference*, 1884–1889. Shanghai, China.
- Pastorino, R., Richiede, D., Cuadrado, J., and Trevisani, A. (2013). State estimation using multibody models and non-linear Kalman filters. *International Journal of Non-Linear Mechanics*, 53, 83–90.
- Puranik, Y., Bavdekar, V.A., Patwardhan, S.C., and Shah, S.L. (2012). An ensemble Kalman filter for systems governed by differential algebraic equations (DAEs). In *Proceedings of the 8th IFAC Symposium on Advanced Control of Chemical Processes*, 531–536. Singapore.
- Purohit, J.L., Patwardhan, S.C., and Mahajani, S.M. (2013). DAE-EKF-based nonlinear predictive control of reactive distillation systems exhibiting input and output multiplicities. *Industrial & Engineering Chemistry Research*, 52(38), 13699–13716.
- Purohit, J.L., Patwardhan, S.C., and Mahajani, S.M. (2015). Performance evaluation of bayesian state estimators for nonlinear DAE systems using a moderately high dimensional reactive distillation column model. In *Proceedings of the 12th International Symposium on Process Systems Engineering and 25th European Symposium on Computer Aided Process Engineering*, 1763–1768. Copenhagen, Denmark.
- Qiu, L., Wang, Y., and Reitz, R.D. (2014). Multiphase dynamic flash simulations using entropy maximization and application to compressible flow with phase change. *AIChE Journal*, 60(8), 3013–3024.
- Ritschel, T.K.S., Capolei, A., Gaspar, J., and Jørgensen, J.B. (2017a). An algorithm for gradient-based dynamic optimization of UV flash processes. *Computers and Chemical Engineering*. In Press. DOI: <https://doi.org/10.1016/j.compchemeng.2017.10.007>.
- Ritschel, T.K.S., Gaspar, J., and Jørgensen, J.B. (2017b). A thermodynamic library for simulation and optimization of dynamic processes. In *Proceedings of the 20th World Congress of the International Federation of Automatic Control*.
- Ritschel, T.K.S., Gaspar, J., Capolei, A., and Jørgensen, J.B. (2016). An open-source thermodynamic software library. Technical Report DTU Compute Technical Report-2016-12, Department of Applied Mathematics and Computer Science, Technical University of Denmark.
- Simon, D. (2006). *Optimal State Estimation: Kalman, H Infinity, and Nonlinear Approaches*. John Wiley & Sons.
- Talebi, H.A., Abdollahi, F., Patel, R.V., and Khorasani, K. (2010). *Neural Network-Based State Estimation of Nonlinear Systems. Application to Fault Detection and Isolation*, volume 395 of *Lecture Notes in Control and Information Sciences*. Springer-Verlag New York.
- Thomson, G.H. (1996). The DIPPR® databases. *International Journal of Thermophysics*, 17(1), 223–232.